DUSP11 Attenuates Lipopolysaccharide-Induced Macrophage Activation by Targeting TAK1

Chia-Yu Yang,*,†,[1] Huai-Chia Chuang,*,[1] Ching-Yi Tsai,* Yu-Zhi Xiao,* Jhih-Yu Yang,* Rou-Huei Huang,* Ying-Chun Shih,* and Tse-Hua Tan*,‡

Dual-specificity phosphatase 11 (DUSP11, also named as PIR1) is a member of the atypical DUSP protein tyrosine phosphatase family. DUSP11 is only known to be an RNA phosphatase that regulates noncoding RNA stability. To date, the role of DUSP11 in immune cell signaling and immune responses remains unknown. In this study, we generated and characterized the immune cell functions of DUSP11-deficient mice. We identified TGF-β–activated kinase 1 (TAK1) as a DUSP11-targeted protein. DUSP11 interacted directly with TAK1, and the DUSP11–TAK1 interaction was enhanced by LPS stimulation in bone marrow–derived macrophages. DUSP11 deficiency enhanced the LPS-induced TAK1 phosphorylation and cytokine production in bone marrow–derived macrophages. Furthermore, DUSP11-deficient mice were more susceptible to LPS-induced endotoxic shock. The LPS-induced serum levels of IL-1β, TNF-α, and IL-6 were significantly elevated in DUSP11-deficient mice compared with those of wild-type mice. The data indicate that DUSP11 inhibits LPS-induced macrophage activation by targeting TAK1. ***The Journal of Immunology*****, 2020, 205: 1644–1652.**

Dual-specificity phosphatases (DUSPs) are a family of protein phosphatases. DUSPs can dephosphorylate both threonine/serine and tyrosine residues in the Thr-X-Tyr (TXY) activation motif of MAPKs (1). The intensity and duration of MAPK activation are negatively regulated by dephosphorylation (2–4). DUSP family phosphatases currently contain 25 members and can be classified into classical or atypical DUSPs based on the presence or absence of the kinase-interacting motif (KIM) (1, 5). Classical DUSPs, also named as MAPK phosphatases (MKPs), contain the KIM motif, an N-terminal Cdc25 homology domain, and a highly conserved C-terminal phosphatase domain. The structure of atypical DUSPs are relatively simpler, contrasting to classical DUSPs; they lack the KIM motif and N-terminal Cdc25 homology domain (5–7).

*Immunology Research Center, National Health Research Institutes, 35053 Zhunan, Taiwan; †Department of Microbiology and Immunology, College of Medicine, Chang Gung University, 33302 Tao-Yuan, Taiwan; and ‡Department of Pathology & Immunology, Baylor College of Medicine, Houston, TX 77030

[1]C.-Y.Y. and H.-C.C. contributed equally to this work.

ORCID: 0000-0003-4969-3170 (T.-H.T.).

Received for publication March 27, 2020. Accepted for publication July 19, 2020.

This work was supported by grants from the National Health Research Institutes, Taiwan (IM-107-PP-01 and IM-107-SP-01 to T.-H.T.) and the Ministry of Science and Technology, Taiwan (MOST-107-2321-B-400-008 and MOST-107-2314-B-400-008 to T.-H.T. and MOST-107-2628-B-400-001 and MOST-108-2314-B-400-015 to H.-C.C.). T.-H.T. is a Taiwan Bio-Development Foundation Chair in Biotechnology.

C.-Y.Y. and H.-C.C. designed and performed experiments, analyzed and interpreted data, and wrote the manuscript; C.-Y.T., Y.-Z.X., J.-Y.Y., R.-H.H., and Y.-C.S. performed experiments; T.-H.T. conceived of the study, supervised experiments, and wrote the manuscript.

Address correspondence and reprint requests to Dr. Tse-Hua Tan, Immunology Research Center, National Health Research Institutes, 35053 Zhunan, Taiwan. E-mail address: ttan@nhri.edu.tw

Abbreviations used in this article: BMDM, bone marrow–derived macrophage; DUSP, dual-specificity phosphatase; DUSP11, dual-specificity phosphatase 11; IKK, IκB kinase; KIM, kinase-interacting motif; KO, knockout; KSHV, Kaposi sarcoma–associated herpesvirus; PLA, proximity ligation assay; qPCR, quantitative PCR; TAK1, TGF-β–activated kinase 1; WT, wild-type.

DUSP 11 (DUSP11, also named RIP1) is an atypical DUSP and is known to be an RNA triphosphatase (8, 9). DUSP11 converts the 5′ triphosphate of microRNA precursors to a 5′ monophosphate and regulates the levels of cellular noncoding RNAs (8–10). During Kaposi sarcoma–associated herpesvirus (KSHV) infection, DUSP11 removes 5′ triphosphates of KSHV vault RNAs and prevents vault RNA recognition by RIG-I, leading to attenuation of KSHV lytic reactivation (11). To date, the functional roles of DUSP11 in the development of immune cells and innate immune responses are still unclear.

TGF-β–activated kinase 1 (TAK1) is a serine/threonine protein kinase and is a member of the MAPK kinase kinase (MAP3K) family (12, 13). TAK1 is activated by various extracellular stimuli such as IL-1β, TNF-α, and TLR signaling. TAK1 transmits the upstream signal from receptor complexes (14) or MAP4Ks (13, 15–17) to the downstream MAP2Ks and IκB kinase (IKK), leading to activation of JNK/p38 and NF-κB.

To investigate the in vivo function of DUSP11 in immune cell signaling and immune responses, a DUSP11-deficient mouse line was generated. In this study, we report that DUSP11 interacts with TAK1 upon LPS signaling in macrophages. Also, DUSP11 deficiency enhances LPS-induced macrophage activation in bone marrow–derived macrophages (BMDMs). DUSP11-deficient mice showed increased susceptibility and cytokine production to LPS-induced endotoxic shock in vivo. In conclusion, our results indicate that DUSP11 inhibits LPS signaling and immune responses by targeting TAK1.

Materials and Methods

Generation of DUSP11-deficient mice

DUSP11 gene deficiency in a 129 mouse embryonic stem cell clone (BB0198) was purchased from the International Gene Trap Consortium. To generate chimeric mice, embryonic stem cells were injected into blastocysts from C57BL/6 mice by the Transgenic Mouse Model Core, National Research Program for Biopharmaceuticals (Taipei, Taiwan). Originally, the extent of DUSP11 deficiency in the mouse line was variable. To solve this problem, mice with efficient DUSP11 deficiency/knockdown were identified and then were used as breeders. The DUSP11-deficient mice in the C57BL/6 background were generated by backcrossing the heterozygous DUSP11 progeny with C57BL/6 mice for more than 10 generations. The

genotypes of mice were determined by a PCR analysis with the common 3′ primer 5′-CGCTGCCCAACTGGGAGATAGTCTTT-3′, the 5′ primer specific for wild-type (WT) allele 5′-GTTAGGCTGTTCTGCTATGGC-3′, and the 5′ primer specific for knockout (KO) allele 5′-GATTGTACTGAGAGTGCACC-3′ mixed together in the same reaction. PCR products were analyzed by electrophoresis, and the DNA fragments with 276 and 200 bp represented the WT and KO alleles, respectively. For detection of DUSP11 mRNA levels by quantitative PCR (qPCR), the primer pair forward, 5′-CTACGGAGCAAGTCTACACC-3′ and reverse, 5′-GCCTCTCTGGTAAACACTCTG-3′ were used. Mice used in this study were 5–12 wk of age. Mice were housed under specific pathogen–free conditions under institutional guidelines, and all animal experiments were approved by the Institutional Animal Care and Use Committee at the National Health Research Institutes.

Cell culture

The HEK293T human embryonic kidney cell line and the Raw264.7 mouse macrophage cell line were cultured in DMEM (Life Technologies) containing 10% FCS plus 10 μg/ml streptomycin and 10 U/ml penicillin. Primary BMDMs from WT and DUSP11-deficient mice were differentiated by the standard procedure. In brief, bone marrow cells from femora and tibiae were flushed with cold PBS and cultured with RPMI 1640 with 10% FCS, 1% penicillin/streptomycin (Life Technologies), and 25 ng/ml M-CSF for 7 d. A total of 2×10^6 BMDMs in six-well plates were stimulated with LPSs (0.1, 0.5, or 1 μg/ml) for 72 h. After LPS stimulation, the culture medium was collected and subjected to ELISA.

Flow cytometry analyses

Thymus, spleen, and lymph nodes were isolated from mice, and cells were mashed and filtered through a 70-μm cell strainer to obtain single-cell suspensions. Cells were depleted of RBCs by RBC lysis buffer. Single-cell suspensions of 1×10^6 cells were stained with the fluorescently labeled anti–CD3-FITC (145-2C11), anti–CD3-PerCP (145-2C11), anti–CD4-Pacific Blue (RM4-5), anti–CD8-allophycocyanin-Cy7 (53-6.7), anti–B220 (RA3–6B2)-PE-Cy7, anti–Gr-1-PE (RB6-8C5), anti–F4/80-PE-Cy7 (BM8), or anti–CD11b-PerCP-Cy5.5 (M1/70) Abs (all from BioLegend) for 15 min at 4°C in 50 μl of staining buffer (1× PBS, 2% FBS, 0.01% NaN_3). The cells were then washed and analyzed on a FACSCanto II flow cytometer (BD Biosciences). The cell populations were analyzed using FlowJo software (BD Biosciences).

Liquid chromatography–mass spectrometry

The sample preparation and liquid chromatography–mass spectrometry analysis performed were as previously described (18).

Plasmids, Abs, and reagents

Flag-DUSP11 plasmid was constructed by subcloning human DUSP11 cDNA into the vector pCMV6-AC-3DDK (OriGene Technologies). Myc-TAK1 plasmid was constructed by subcloning human TAK1 cDNA into the vector pCMV6-AC-Flag (OriGene Technologies). Flag-DUSP14 plasmid was constructed by subcloning human DUSP14 cDNA into the vector pCMV6-AC-3DDK (OriGene Technologies) as described previously (19). The Abs specific for TGF-β–activated kinase 1–binding protein 1 (TAB1), TAK1, phospho-TAK (pS412), JNK, phospho-JNK (pT183/pY185), IKKβ, and phospho-IKK were purchased from Cell Signaling Technology. The Ab recognizing both human and murine DUSP11 was generated by immunization of a rabbit with peptides (murine DUSP11 epitope ^{229}TNNKPVKKKPRKNRRGGHL^{247}). Anti-Flag (DDK) Ab was purchased from Origene Technologies. Anti-vinculin Ab was purchased from Merck. The Abs for Myc, tubulin, and actin were purchased from Sigma-Aldrich. LPS (*Escherichia coli* serotype O1111:B4) and DMSO were obtained from Sigma-Aldrich.

Coimmunoprecipitation and Western blotting analysis

Cell lysate was lysed in lysis buffer (50 mM Tris–Cl [pH 7.4], 150 mM NaCl, 5 mM EDTA, 0.1% Triton X-100, 0.02% NaN_3, 100 mM PMSF, 1 M sodium fluoride, 0.5 mg/ml leupeptin, 1 mg/ml aprotinin, and 5 mg/ml pepstatin A) at 4°C for 30 min. For coimmunoprecipitation, cell lysates were incubated with anti-Myc agarose beads (9E10; Sigma-Aldrich) or anti-Flag agarose beads (M2; Sigma-Aldrich) in 1 ml of lysis buffer at 4°C for 2 h. The immunocomplexes were washed three times with lysis buffer, followed by Western blotting analysis. For Western blotting analysis, the lysates were boiled at 95°C for 5 min and then subjected to SDS-PAGE, and the separated proteins were transferred to a PVDF membrane and blocked with Tris-buffered saline with 0.1% Tween 20 containing 5% BSA for 1 h. The PVDF membrane was incubated with specific primary Abs at 4°C overnight, followed by incubation with HRP-conjugated secondary Abs at room temperature for 1 h. The specific signals were detected by an ECL Substrate Kit (Millipore).

LPS-induced endotoxic shock

Six- to twelve-week-old DUSP11 WT or DUSP11-deficient mice were i.p. injected with LPS (15 mg/kg body weight) in PBS to induce endotoxic shock and were monitored for survival over 5 d. For measurement the serum cytokine production, blood samples were obtained from mice 6 h after LPS injection. The blood samples were centrifuged at 18,000 × *g* for 15 min at room temperature. The supernatants were stored at −80°C until they were assayed for cytokines by ELISA.

ELISA

The levels of TNF-α, IL-1β, and IL-6 in cell supernatants or mouse sera were quantified using ELISA Kits (eBioscience) according to the manufacturer's instructions.

Proximity ligation assay

In situ proximity ligation assay (PLA) analyses were performed as previously described using the Duolink In Situ Red Starter Kit (Sigma-Aldrich) according to the manufacturer's instructions (20). Briefly, WT and DUSP11 KO BMDMs were stimulated with LPS at the indicated time, and then the cells were deposited on the glass slides and pretreated with fixation and blocking solutions. Cells were then incubated with primary Abs against DUSP11 and TAK1, followed by oligonucleotide (PLA Probe MINUS or PLA Probe PLUS)-conjugated secondary Abs. After ligation and amplification reactions, the slides were washed and mounted using a Duolink In Situ Mounting Medium with DAPI. The PLA signals from paired DUSP11 and TAK1 in close proximity (<40 nm) were visualized as individual red dots by a fluorescence microscope (DM2500; Leica). Red dots represent direct interactions. To analyze the results, the number of red dots and DAPI-positive cells were counted per field. The PLA signal was quantified and was shown as the number of PLA (red) signals per DAPI (blue)-positive cells.

In vitro phosphatase assay

Flag-tagged TAK1 proteins were immunoprecipitated from lysates of HEK293T cells transfected with Flag-TAK1 plasmid. Immunoprecipitated TAK1 proteins were incubated with immunoprecipitated DUSP11 WT or DUSP11 mutant (Cys^{152} to Ser^{152}) proteins for 2 h. The reaction products were boiled in 5× sample buffer, followed by Western blotting with anti–phospho-TAK1 Ab.

Results

Normal lymphoid organ development in DUSP11-deficient mice

The DUSP11-deficient mice were generated for studying the function of DUSP11 in immune cell development and immune responses. An insertion vector containing a splice acceptor, β-geo (a fusion of β-galactosidase and neomycin resistance genes), and a polyadenylation sequence was inserted into the intron between exon 1 and exon 2 of the targeted DUSP11 allele (Fig. 1A). Successful targeting of DUSP11 was validated by PCR analysis of genomic DNAs from mouse tails (Fig. 1B). qPCR analysis using paired primers targeting DUSP11 at exon 9 confirmed the loss of DUSP11 mRNA expression in the peripheral blood, thymus, spleen, and lymph node of DUSP11-deficient mice (Fig. 1C).

We next examined whether loss of DUSP11 expression might alter the development of immune cells in DUSP11-deficient mice. Flow cytometry analysis showed that DUSP11 deficiency did not alter the development of $CD4^-CD8^-$ double-negative, $CD4^+CD8^+$ double-positive, $CD8^+$ single-positive, or $CD4^+$ single-positive thymocytes (Fig. 2A). The data also showed similar proportions of $CD3^+$ T cells, $CD4^+$ T cells, $CD8^+$ T cells, and $B220^+$ B cells in the spleen and lymph nodes of WT and DUSP11-deficient mice (Fig. 2B, 2C). The frequencies of macrophages ($F4/80^+CD11b^+$) and neutrophils ($Gr\text{-}1^+CD11b^+$) in the spleen were also similar in

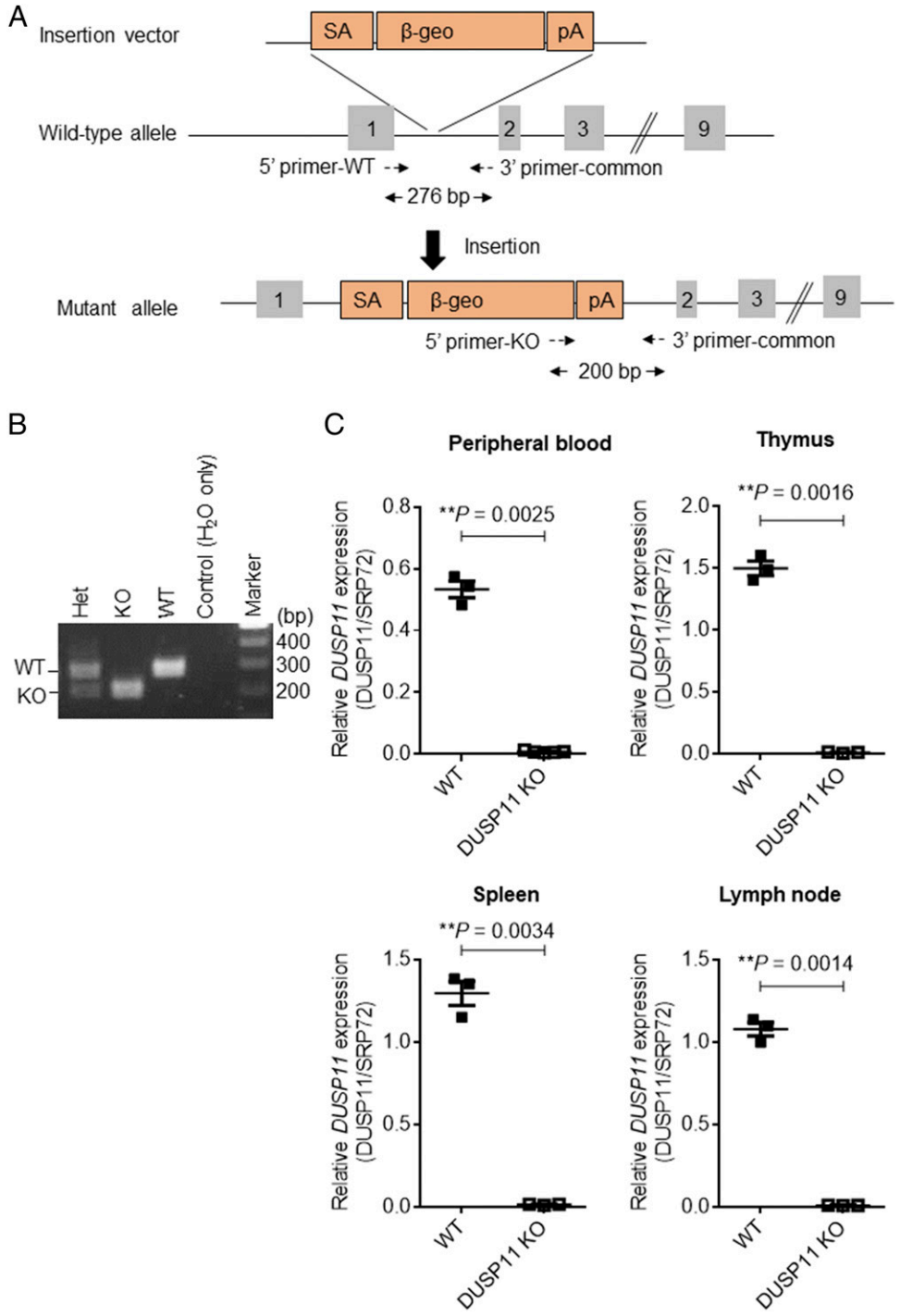

FIGURE 1. Generation of the DUSP11-deficient mice. (**A**) The structure of the gene-trap vector. The boxes with individual numbers are the individual exons of DUSP11; dotted arrows are the primers for PCR. (**B**) Genotyping of mice from the progeny of "heterozygous-by-heterozygous" mating. The PCR products of the 270-bp band indicate the WT allele and the PCR products of the 200-bp band indicate the DUSP11-deficient (KO) allele. (**C**) A qPCR analysis of mRNAs from peripheral blood cells, thymus, spleen, and lymph nodes from WT and DUSP11-deficient (DUSP11 KO) mice. Data shown are representative of three independent experiments. β-geo, fusion of β-galactosidase and neomycin resistance genes; Het, heterozygote; pA, polyadenylation; SA, splice acceptor site.

WT and DUSP11-deficient mice (Fig. 2D). These data suggest that DUSP11 is not essential for the immune cell development.

DUSP11 inducibly interacts with TAK1 upon LPS signaling in macrophages

We then searched for the potential target(s) of DUSP11 using DUSP11 immunocomplexes by coimmunoprecipitation and liquid chromatography–mass spectrometry. HEK293T cells were transfected with Flag-DUSP11, and DUSP11-interacting proteins were coimmunoprecipitated with anti-Flag Ab. The immunocomplexes were fractionated by SDS-PAGE. The protein bands were excised and subjected to liquid chromatography–mass spectrometry. We identified TAK1 as a DUSP11-interacting protein by mass spectrometry (Fig. 3A). The interaction of DUSP11 with TAK1 was confirmed by reciprocal coimmunoprecipitation assays using Myc-DUSP11–overexpressing and Flag-TAK1–overexpressing

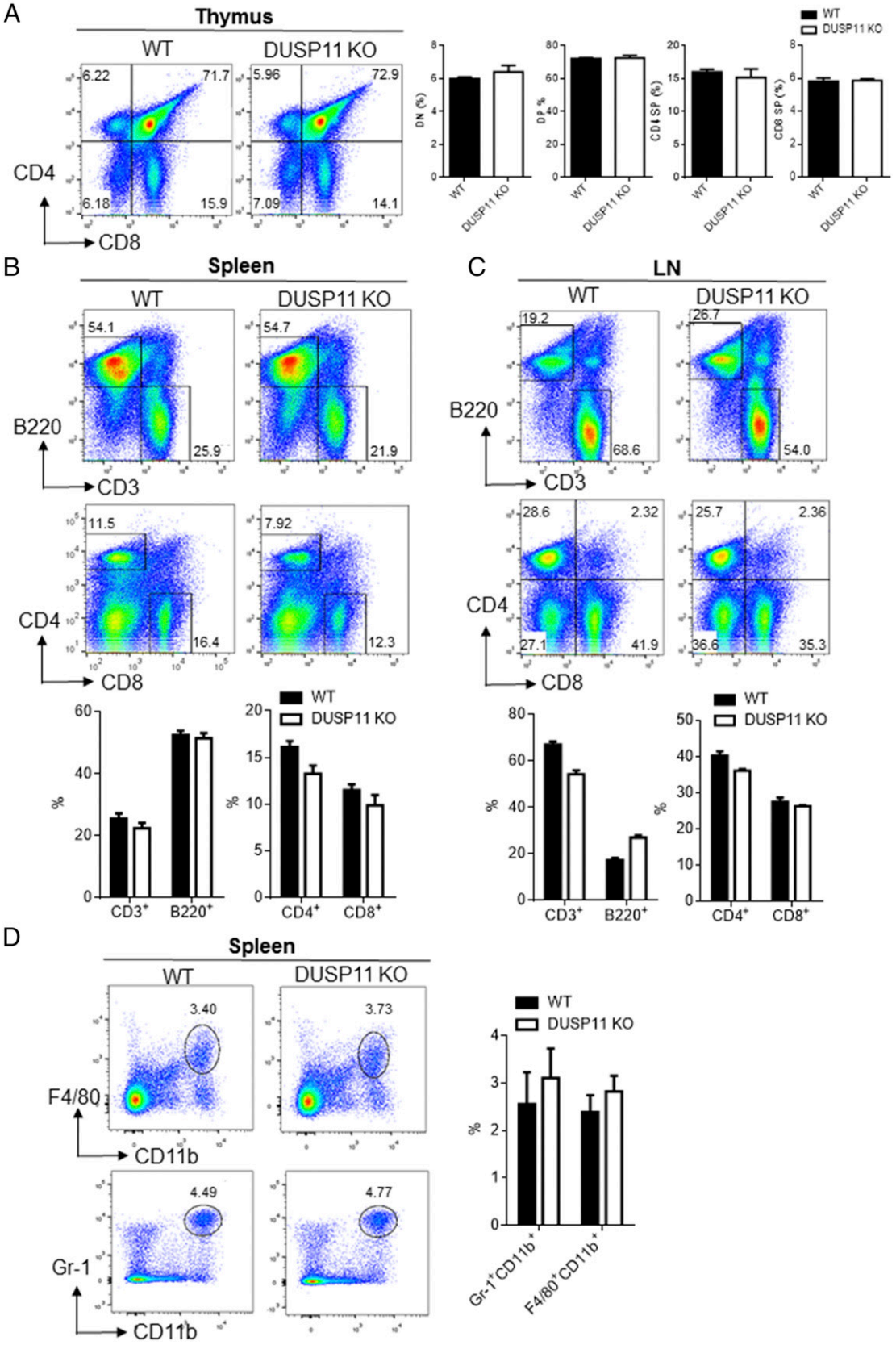

FIGURE 2. Normal lymphoid organ development in DUSP11-deficient mice (DUSP11 KO). Thymocytes from WT and DUSP11 KO mice were stained for CD4 and CD8 and analyzed by flow cytometry (**A**). Spleens (**B**) and lymph nodes (**C**) from WT and DUSP11 KO mice were stained for CD4, CD8, CD3, and B220 and analyzed by flow cytometry. (**D**) Splenic cells from WT and DUSP11 KO mice were stained for F4/80, CD11b, and Gr-1. Percentage of $CD1b^+F4/80^+$ cells (macrophages) or $CD11b^+Gr\text{-}1^+$ cells (neutrophils) within each quadrant is shown on the plots. Data are presented as mean ± SEM. The statistical difference between WT and DUSP11 KO mice were performed with an unpaired *t* test. Data shown are representative of three independent experiments. A p value <0.05 was considered statistically significant.

HEK293T cell lysates (Fig. 3B). Furthermore, HEK293T cells were transfected with Flag-DUSP11 or Flag-DUSP14 plasmid. The immunocomplexes were coimmunoprecipitated with anti-Flag Ab and then analyzed by Western blotting. The results demonstrated that DUSP11 interacts with endogenous TAK1 but not endogenous TAB1 proteins (Fig. 3C). In contrast, consistent with our previous findings (19), DUSP14 directly interacted with endogenous TAB1 proteins but not endogenous TAK1 proteins, as detected by coimmunoprecipitation assay (Fig. 3C).

Next, we asked whether DUSP11 dephosphorylates TAK1 in vitro. HEK293T cells were transfected with Flag-TAK1 plasmid, and then TAK1 proteins were purified by immunoprecipitation with

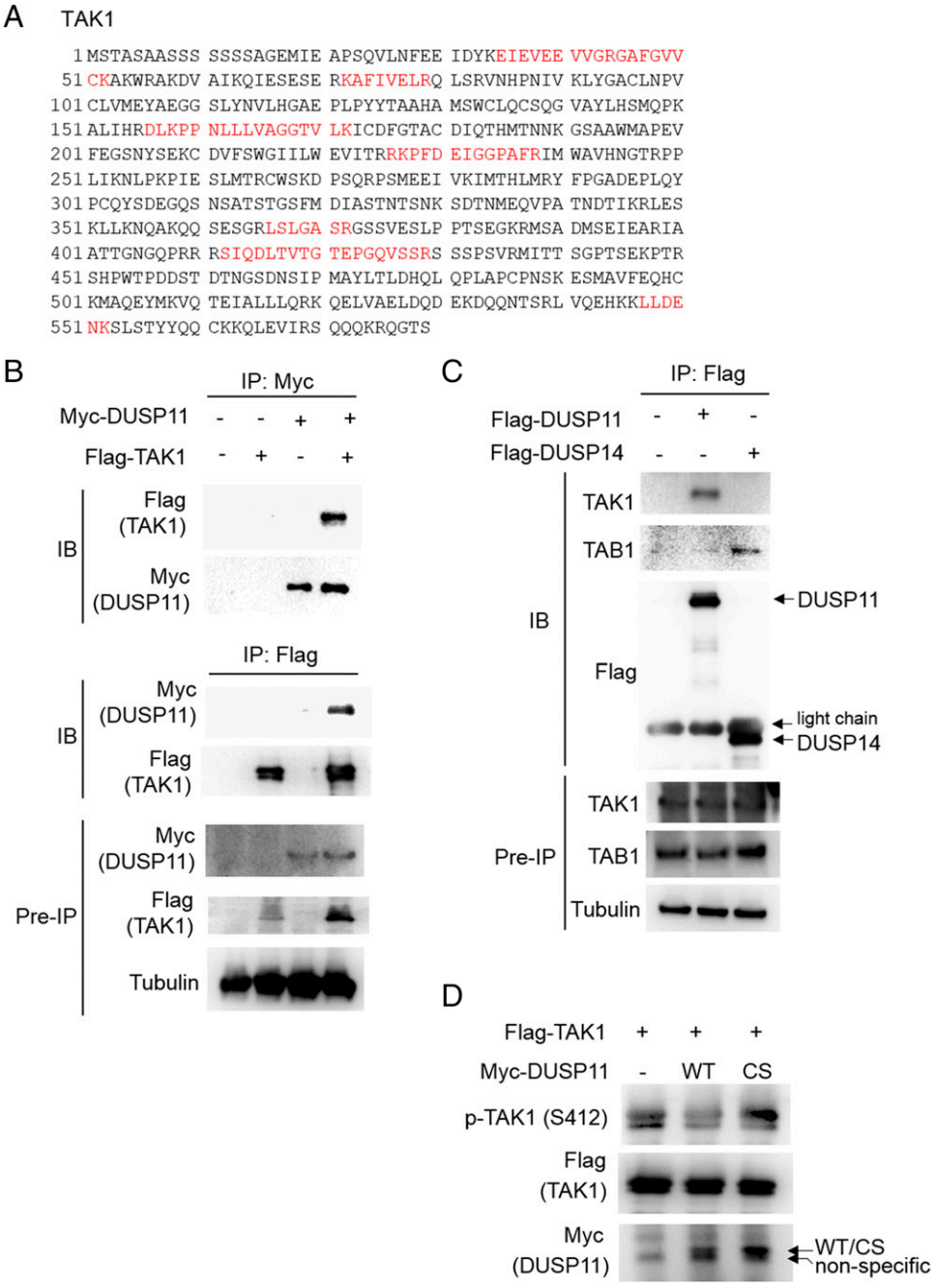

FIGURE 3. TAK1 is a DUSP11-interacting protein. DUSP11 interacts with TAK1 in HEK293T identified by coimmunoprecipitation and mass spectrometry. (**A**) Sequence of the DUSP11-interacting protein TAK1. Seven human TAK1 peptides (red) were identified by mass spectrometry–based proteomics using DUSP11 immunocomplexes. (**B**) DUSP11 interacts with TAK1 in HEK293T cells. Coimmunoprecipitation of DUSP11 and TAK1 proteins using lysates of HEK293T cells transfected with empty vector or plasmid encoding Myc-DUSP11 with or without plasmid encoding Flag-TAK1. (**C**) DUSP11 interacts with endogenous TAK1 in HKE293T cells. Cells were transfected with empty vector or plasmid encoding Flag-DUSP11 or Flag-DUSP14. Coimmunoprecipitation with an anti-Flag Ab, followed by Western blotting analysis of DUSP11, DUSP14, TAK1, and TAB1. (**D**) In vitro phosphatase assays of purified DUSP11 WT or phosphatase-dead mutant (Cys^{152} to Ser^{152}), using purified Flag-TAK1 as substrates. Data shown are representative of three independent experiments.

anti-Flag Ab. The purified Myc-DUSP11 WT proteins dephosphorylated the purified Flag-TAK1 proteins at Ser412 residue, whereas the phosphatase-dead DUSP11 mutant (Cys^{152} to serine) proteins did not dephosphorylate TAK1 using in vitro phosphatase assays (Fig. 3D).

TAK1 is an essential mediator that transmits the TLR4 signal from the receptor complex to downstream effectors IKK and MAPKs, which control the production of inflammatory cytokines important for innate immunity. To determine whether DUSP11 regulates TAK1 activation during LPS signaling, we investigated the potential interaction between DUSP11 and TAK1 upon LPS stimulation in macrophages by coimmunoprecipitation assays and PLA. Raw264.7 macrophages were cotransfected with Flag-DUSP11 plus Myc-TAK1 plasmids and then stimulated with LPS at the indicated time. The results showed that DUSP11 modestly interacted with TAK1 without LPS stimulation when both proteins were overexpressed (Fig. 4A). The interaction between DUSP11 and TAK1 was further enhanced by LPS stimulation in Raw 264.7 macrophages detected by coimmunoprecipitation assays (Fig. 4A). Moreover, the LPS-induced interaction between endogenous DUSP11 and TAK1 proteins in BMDMs were confirmed by PLA (Fig. 4B, 4C). The anti-DUSP11 Ab specificity for PLA signals was validated using DUSP11-deficient BMDMs (Fig. 4B, 4C). Collectively, the data suggest that DUSP11 directly interacts with TAK1 in BMDMs during TLR signaling.

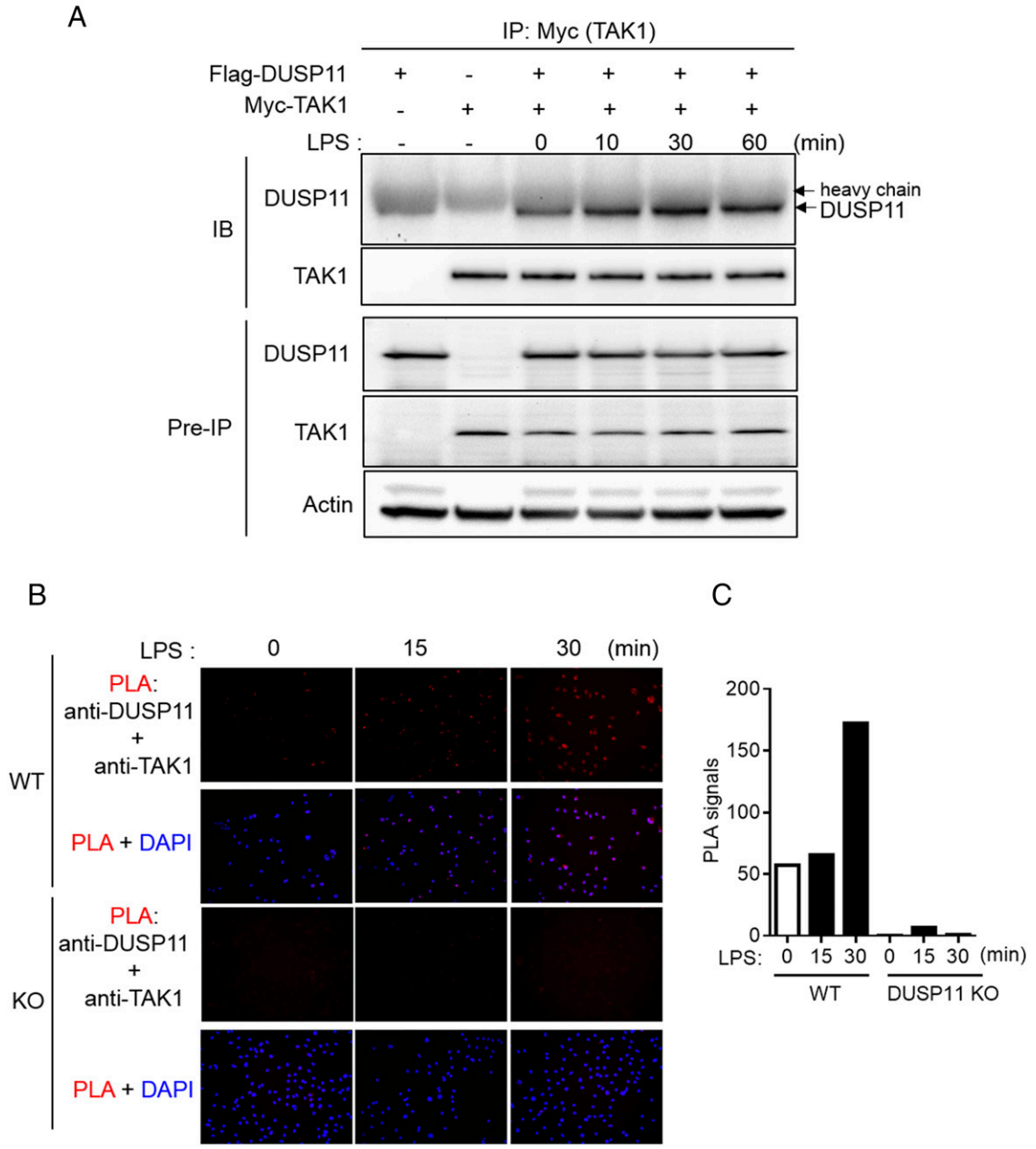

FIGURE 4. DUSP11 interacts with TAK1 upon LPS signaling in macrophages. (**A**) DUSP11 interacts with TAK1 in Raw264.7 macrophages. Coimmunoprecipitation and immunoblot analysis of DUSP11 and TAK1 in lysates of Raw264.7 macrophages transfected with plasmid encoding Flag-DUSP11 and Myc-TAK1. (**B**) BMDMs were generated from WT or DUSP11-deficient (DUSP11 KO) mice. The interaction of DUSP11 with TAK1 upon 5 μg/ml LPS stimulation at 15 and 30 min were detected with in situ PLAs. Original magnification ×400. (**C**) In PLA assays, red dots represent direct interactions. The numbers of red dots and DAPI-positive cells were counted per field. The PLA signal was quantified and was shown as the number of PLA (red) signals per DAPI (blue)-positive cells. Data shown are representative of three independent experiments.

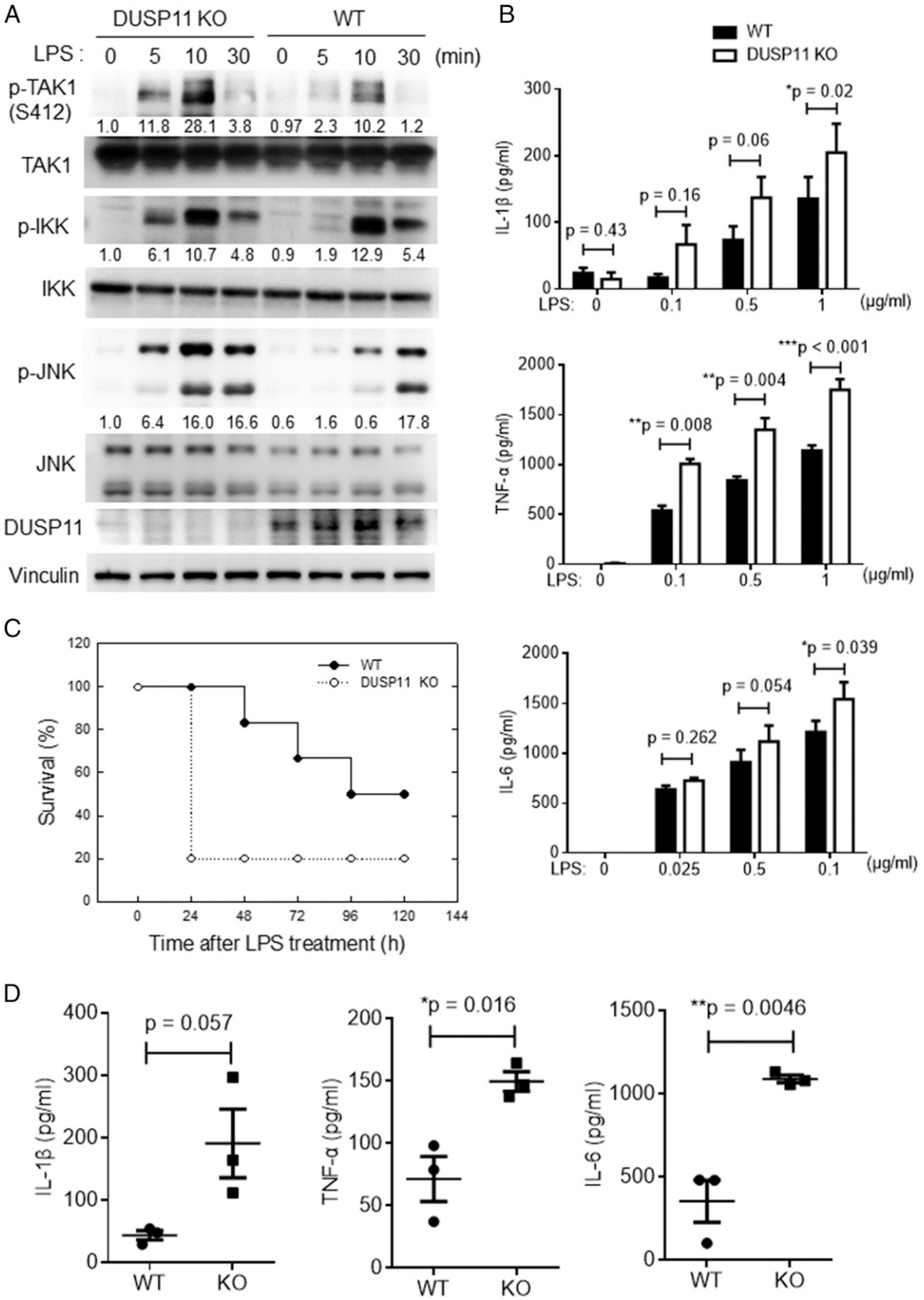

FIGURE 5. DUSP11-deficient mice are more susceptible to LPS-induced endotoxic shock. (**A**) BMDMs from WT and DUSP11-deficient (DUSP11 KO) mice were stimulated with LPS at the indicated time. The cells were lysed; the lysates were immunoblotted with Abs to phospho-TAK1 (Ser412), TAK1, phospho-IKK, IKKβ, phospho-JNK, JNK, and vinculin. The relative phosphorylation levels (phosphorylated protein level/total protein level) were determined by densitometry analysis. (**B**) BMDMs from WT and DUSP11 KO mice were stimulated with LPS at indicated concentrations for 72 h. Levels of IL-1β, TNF-α, and IL-6 were measured by ELISA. (**C**) Mortality after LPS-induced septic shock in mice. LPS was i.p. injected at the dosage of 15 mg/kg body weight. Closed circle represents WT ($n = 6$); open circle represents DUSP11 KO mice ($n = 5$). (**D**) After LPS stimulation for 6 h, the sera from WT and DUSP11 KO mice were collected, and the concentrations of IL-1β, TNF-α, and IL-6 in the sera of WT and DUSP11 KO mice were determined by ELISA. Data are presented as mean ± SEM. Data shown are representative of three independent experiments. $*p < 0.05$, $**p < 0.01$, $***p < 0.001$.

DUSP11 deficiency enhances TAK1 phosphorylation and exacerbates LPS-induced endotoxic shock

During LPS signaling, the phosphorylation of TAK1 is required for its kinase activity, leading to induction of proinflammatory cytokines. We further characterized the levels of phosphorylated TAK1 in DUSP11-deficient BMDMs upon LPS stimulation. Our results showed that the phosphorylation levels of TAK1 at Ser412 were significantly increased in DUSP11-deficient BMDMs compared with those of WT BMDMs (Fig. 5A). Also, the phosphorylation of IKK and JNK were also enhanced in DUSP11-deficient BMDMs (Fig. 5A). We characterized the proinflammatory cytokine production in DUSP11-deficient BMDMs upon LPS stimulation. Our results showed that levels of IL-1β, TNF-α, and IL-6 were significantly higher in DUSP11-deficient BMDMs than those of WT controls (Fig. 5B). We next examined whether DUSP11 deficiency could increase the susceptibility to LPS-induced endotoxic shock in vivo. WT and DUSP11-deficient mice were i.p. injected with 15 mg/kg body weight LPS and monitored for 120 h. All of the mice that received LPS treatment showed apparent signs of distress such as apathy, fur ruffling, and diarrhea. The data appear to suggest that DUSP11-deficient mice are more susceptible to endotoxic shock (Fig. 5C). In contrast, WT mice did not die until 48 h after LPS injection, and 40% of the WT mice still survived at 120 h (Fig. 5C). Furthermore, serum levels of IL-1β, TNF-α, and IL-6 were significantly higher in DUSP11-deficient mice than those in WT mice at 6 h after LPS injection (Fig. 5D).

Discussion

DUSP11 has been previously reported as an RNA phosphatase (8, 9). In this study, we demonstrated that in addition to targeting to RNAs, DUSP11 is an important phosphatase that directly interacts with and regulates TAK1 activation in macrophages, leading to the reduction of LPS-induced endotoxic shock. LPS-mediated signaling pathways have been shown to stimulate the production of proinflammatory cytokines, such as TNF-α, IL-6, and IL-1β; the overproduction of these proinflammatory cytokines contributes to the induction of endotoxic shock. The serum levels of TNF-α, IL-6, and IL-1β were significantly elevated in DUSP11-deficient mice compared with those of WT mice upon LPS challenge.

After TLR4 ligand stimulation, the MyD88-dependent pathways were activated, leading to sequential activation of IL-1R–associated kinase (IRAK1), IRAK4, TNFR-associated factor 6 (TRAF6), and TAK1 (14). Furthermore, phosphorylation and ubiquitination of TAK1 and its binding partners TAB1 and TAB2/3 are essential for TAK1 activation (21, 22). TAK1 Ser412 phosphorylation is regulated by X-linked protein kinase (PRKX) and cAMP-dependent protein kinase catalytic subunit α (PKACα) under TLR signaling (23). Conversely, the phosphatase holoenzyme PP1 negatively regulates TAK1 Ser412 phosphorylation in TLR signaling (24). In this report, we showed that DUSP11 directly interacted with and dephosphorylated the TAK1 protein as its substrate, leading to inactivation of TAK1 downstream molecules (IKK and JNK). Another DUSP family member, DUSP14, attenuates activation of the TAB1–TAK1 signaling through directly targeting TAB1 in T cells (18, 19). Unlike DUSP14, DUSP11 bound to TAK1 but not TAB1. DUSP14 phosphatase activity is induced by its protein methylation and ubiquitination under TCR signaling (18, 19, 25); therefore, it would be interesting to study whether and how DUSP11 activity is regulated by its upstream regulators upon TLR signaling. Furthermore, it is important to characterize the structure–function relationships between DUSP11 and TAK1 in immune cells upon TLR signaling. Besides DUSP11 and DUSP14, several DUSP family members play important roles in immune cell activation, inflammatory responses (6, 7, 26–32), or tumorigenesis (33–35). These findings suggest that DUSP family members have individual functions, instead of redundant roles, in regulation of various immune cell signaling pathways.

Acknowledgments

We thank the Laboratory Animal Center (Association for Assessment and Accreditation of Laboratory Animal Care International accredited) of the National Health Research Institutes for mouse housing. We thank the Transgenic Mouse Model Core of National Research Program for Biopharmaceuticals for blastocyst microinjection and generation of DUSP11 KO mice. We thank the Institute of Biological Chemistry of Academia Sinica for mass spectrometry–based proteomics.

Disclosures

The authors have no financial conflicts of interest.

References

1. Huang, C. Y., and T. H. Tan. 2012. DUSPs, to MAP kinases and beyond. *Cell Biosci.* 2: 24.
2. Chen, Y. R., C. F. Meyer, and T. H. Tan. 1996. Persistent activation of c-Jun N-terminal kinase 1 (JNK1) in γ radiation-induced apoptosis. *J. Biol. Chem.* 271: 631–634.
3. Chen, Y. R., X. Wang, D. Templeton, R. J. Davis, and T. H. Tan. 1996. The role of c-Jun N-terminal kinase (JNK) in apoptosis induced by ultraviolet C and γ radiation. Duration of JNK activation may determine cell death and proliferation. *J. Biol. Chem.* 271: 31929–31936.
4. Chen, Y. R., and T. H. Tan. 2000. The c-Jun N-terminal kinase pathway and apoptotic signaling (review). *Int. J. Oncol.* 16: 651–662.
5. Jeffrey, K. L., M. Camps, C. Rommel, and C. R. Mackay. 2007. Targeting dual-specificity phosphatases: manipulating MAP kinase signalling and immune responses. *Nat. Rev. Drug Discov.* 6: 391–403.
6. Chen, H. F., H. C. Chuang, and T. H. Tan. 2019. Regulation of dual-specificity phosphatase (DUSP) ubiquitination and protein stability. *Int. J. Mol. Sci.* 20: 2668.
7. Lang, R., and F. A. M. Raffi. 2019. Dual-specificity phosphatases in immunity and infection: an update. *Int. J. Mol. Sci.* 20: 2710.
8. Yuan, Y., D. M. Li, and H. Sun. 1998. PIR1, a novel phosphatase that exhibits high affinity to RNA. ribonucleoprotein complexes. *J. Biol. Chem.* 273: 20347–20353.
9. Burke, J. M., and C. S. Sullivan. 2017. DUSP11 - an RNA phosphatase that regulates host and viral non-coding RNAs in mammalian cells. *RNA Biol.* 14: 1457–1465.
10. Burke, J. M., R. P. Kincaid, R. M. Nottingham, A. M. Lambowitz, and C. S. Sullivan. 2016. DUSP11 activity on triphosphorylated transcripts promotes Argonaute association with noncanonical viral microRNAs and regulates steady-state levels of cellular noncoding RNAs. *Genes Dev.* 30: 2076–2092.
11. Zhao, Y., X. Ye, W. Dunker, Y. Song, and J. Karijolich. 2018. RIG-I like receptor sensing of host RNAs facilitates the cell-intrinsic immune response to KSHV infection. *Nat. Commun.* 9: 4841.
12. Yamaguchi, K., K. Shirakabe, H. Shibuya, K. Irie, I. Oishi, N. Ueno, T. Taniguchi, E. Nishida, and K. Matsumoto. 1995. Identification of a member of the MAPKKK family as a potential mediator of TGF-β signal transduction. *Science* 270: 2008–2011.
13. Wang, W., G. Zhou, M. C. Hu, Z. Yao, and T. H. Tan. 1997. Activation of the hematopoietic progenitor kinase-1 (HPK1)-dependent, stress-activated c-Jun N-terminal kinase (JNK) pathway by transforming growth factor β (TGF-β)-activated kinase (TAK1), a kinase mediator of TGF β signal transduction. *J. Biol. Chem.* 272: 22771–22775.
14. Ajibade, A. A., H. Y. Wang, and R. F. Wang. 2013. Cell type-specific function of TAK1 in innate immune signaling. *Trends Immunol.* 34: 307–316.
15. Zhou, G., S. C. Lee, Z. Yao, and T. H. Tan. 1999. Hematopoietic progenitor kinase 1 is a component of transforming growth factor β-induced c-Jun N-terminal kinase signaling cascade. *J. Biol. Chem.* 274: 13133–13138.
16. Yao, Z., G. Zhou, X. S. Wang, A. Brown, K. Diener, H. Gan, and T. H. Tan. 1999. A novel human STE20-related protein kinase, HGK, that specifically activates the c-Jun N-terminal kinase signaling pathway. *J. Biol. Chem.* 274: 2118–2125.
17. Chuang, H. C., X. Wang, and T. H. Tan. 2016. MAP4K family kinases in immunity and inflammation. *Adv. Immunol.* 129: 277–314.
18. Yang, C. Y., L. L. Chiu, C. C. Chang, H. C. Chuang, and T. H. Tan. 2018. Induction of DUSP14 ubiquitination by PRMT5-mediated arginine methylation. *FASEB J.* 32: fj201800244RR.
19. Yang, C. Y., J. P. Li, L. L. Chiu, J. L. Lan, D. Y. Chen, H. C. Chuang, C. Y. Huang, and T. H. Tan. 2014. Dual-specificity phosphatase 14 (DUSP14/MKP6) negatively regulates TCR signaling by inhibiting TAB1 activation. *J. Immunol.* 192: 1547–1557.
20. Chuang, H. C., C. Y. Tsai, C. H. Hsueh, and T. H. Tan. 2018. GLK-IKKβ signaling induces dimerization and translocation of the AhR-RORγt

complex in IL-17A induction and autoimmune disease. *Sci. Adv.* 4: eaat5401
21. Ono, K., T. Ohtomo, S. Sato, Y. Sugamata, M. Suzuki, N. Hisamoto, J. Ninomiya-Tsuji, M. Tsuchiya, and K. Matsumoto. 2001. An evolutionarily conserved motif in the TAB1 C-terminal region is necessary for interaction with and activation of TAK1 MAPKKK. *J. Biol. Chem.* 276: 24396–24400.
22. Scholz, R., C. L. Sidler, R. F. Thali, N. Winssinger, P. C. Cheung, and D. Neumann. 2010. Autoactivation of transforming growth factor β-activated kinase 1 is a sequential bimolecular process. *J. Biol. Chem.* 285: 25753–25766.
23. Ouyang, C., L. Nie, M. Gu, A. Wu, X. Han, X. Wang, J. Shao, and Z. Xia. 2014. Transforming growth factor (TGF)-β-activated kinase 1 (TAK1) activation requires phosphorylation of serine 412 by protein kinase A catalytic subunit α (PKACα) and X-linked protein kinase (PRKX). *J. Biol. Chem.* 289: 24226–24237.
24. Gu, M., C. Ouyang, W. Lin, T. Zhang, X. Cao, Z. Xia, and X. Wang. 2014. Phosphatase holoenzyme PP1/GADD34 negatively regulates TLR response by inhibiting TAK1 serine 412 phosphorylation. *J. Immunol.* 192: 2846–2856.
25. Yang, C. Y., L. L. Chiu, and T. H. Tan. 2016. TRAF2-mediated Lys63-linked ubiquitination of DUSP14/MKP6 is essential for its phosphatase activity. *Cell. Signal.* 28: 145–151.
26. Li, J. P., C. Y. Yang, H. C. Chuang, J. L. Lan, D. Y. Chen, Y. M. Chen, X. Wang, A. J. Chen, J. W. Belmont, and T. H. Tan. 2014. The phosphatase JKAP/DUSP22 inhibits T-cell receptor signalling and autoimmunity by inactivating Lck. *Nat. Commun.* 5: 3618.
27. Ruan, J. W., S. Statt, C. T. Huang, Y. T. Tsai, C. C. Kuo, H. L. Chan, Y. C. Liao, T. H. Tan, and C. Y. Kao. 2016. Dual-specificity phosphatase 6 deficiency regulates gut microbiome and transcriptome response against diet-induced obesity in mice. *Nat. Microbiol.* 2: 16220.
28. Hsu, W. C., M. Y. Chen, S. C. Hsu, L. R. Huang, C. Y. Kao, W. H. Cheng, C. H. Pan, M. S. Wu, G. Y. Yu, M. S. Hung, et al. 2018. DUSP6 mediates T cell receptor-engaged glycolysis and restrains T_{FH} cell differentiation. *Proc. Natl. Acad. Sci. USA* 115: E8027–E8036.
29. Hsiao, W. Y., Y. C. Lin, F. H. Liao, Y. C. Chan, and C. Y. Huang. 2015. Dual-specificity phosphatase 4 regulates STAT5 protein stability and helper T cell polarization. *PLoS One* 10: e0145880.
30. Chuang, H. C., Y. M. Chen, W. T. Hung, J. P. Li, D. Y. Chen, J. L. Lan, and T. H. Tan. 2016. Downregulation of the phosphatase JKAP/DUSP22 in T cells as a potential new biomarker of systemic lupus erythematosus nephritis. *Oncotarget* 7: 57593–57605.
31. Chuang, H. C., and T. H. Tan. 2019. MAP4K family kinases and DUSP family phosphatases in T-cell signaling and systemic lupus erythematosus. *Cells* 8: 1433.
32. Huang, C. Y., Y. C. Lin, W. Y. Hsiao, F. H. Liao, P. Y. Huang, and T. H. Tan. 2012. DUSP4 deficiency enhances CD25 expression and $CD4^+$ T-cell proliferation without impeding T-cell development. *Eur. J. Immunol.* 42: 476–488.
33. Lin, H. P., H. M. Ho, C. W. Chang, S. D. Yeh, Y. W. Su, T. H. Tan, and W. J. Lin. 2019. DUSP22 suppresses prostate cancer proliferation by targeting the EGFR-AR axis. *FASEB J.* 33: 14653–14667.
34. Chen, Y. R., H. C. Chou, C. H. Yang, H. Y. Chen, Y. W. Liu, T. Y. Lin, C. L. Yeh, W. T. Chao, H. H. Tsou, H. C. Chuang, and T. H. Tan. 2017. Deficiency in VHR/DUSP3, a suppressor of focal adhesion kinase, reveals its role in regulating cell adhesion and migration. *Oncogene* 36: 6509–6517.
35. Li, J. P., Y. N. Fu, Y. R. Chen, and T. H. Tan. 2010. JNK pathway-associated phosphatase dephosphorylates focal adhesion kinase and suppresses cell migration. *J. Biol. Chem.* 285: 5472–5478.